JEE Journal of Ecological Engineering

Journal of Ecological Engineering, 25(12), 26–38
https://doi.org/10.12911/22998993/193587
ISSN 2299–8993, License CC-BY 4.0

Received: 2024.09.04
Accepted: 2024.10.20
Published: 2024.11.01

Enhancing the Removal of Methyl Orange Dye by Electrocoagulation System with Nickel Foam Electrode – Optimization with Surface Response Methodology

Amor T. Mohammed Ali[1], Rasha H. Salman[1*]

[1] Department of Chemical Engineering, College of Engineering, University of Baghdad, Baghdad, Iraq
* Corresponding author's e-mail: rasha.habeeb@coeng.uobaghdad.edu.iq

ABSTRACT

Azo dyes like methyl orange (MO) are very toxic components due to their recalcitrant properties which makes their removal from wastewater of textile industries a significant issue. The present study aimed to study their removal by utilizing aluminum and Ni foam (NiF) as anodes besides Fe foam electrodes as cathodes in an electrocoagulation (EC) system. Primary experiments were conducted using two Al anodes, two NiF anodes, or Al-NiF anodes to predict their advantages and drawbacks. It was concluded that the Al-NiF anodes were very effective in removing MO dye without long time of treatment or Ni leaching at in the case of adopting the Al-Al or NiF-NiF anodes, respectively. The structure and surface morphology of the NiF electrode were investigated by energy dispersive X-ray (EDX), and field emission scanning electron microscopy (FESEM). Response surface methodology was utilized to predict the optimum conditions by considering current density with 4–8 mA/cm^2 range, NaCl concentration in the range of 0.5–1 g/L, and electrolysis time of 10–30 min as controlling parameters. A very high MO dye removal percentage was achieved (97.74%) at 8 mA/cm^2, 1 g/L of NaCl within 30 min of electrolysis and consumed energy was 36.299 kWh/kg. This cost-effective EC system with the Al-NiF anodes besides Fe foam as cathode approved its high efficiency in removing MO dye with moderate amounts of NaCl due to the excellent 3D structure of these foam electrodes which highlight foam electrodes as an excellent choice for EC system in an environmentally friendly pathway.

Keywords: electrocoagulation, Ni foam, Fe foam, aluminum, surface response.

INTRODUCTION

Freshwater is currently in low supply worldwide, especially in poor countries. Numerous factors, including overcrowding, urbanization, industrialization, deforestation, agriculture, and the consequences of climate change, are responsible for this shortage of water supplies (Bassyouni et al., 2023). In addition, a lot of the waste from the industries which employ a variety of dyes ends up in waterways. Numerous chemically stable and non-biodegradable colors are present in high concentrations in textile industry waste, which can make treatment difficult (Maruthanayagam et al., 2020). The water contaminated with dyes is thought to pose a serious threat to human health since many organic and inorganic dyes release toxic and carcinogenic byproducts (Salman et al., 2024). The dyeing and finishing procedures used in the textile industry use a lot of water. It has been stated that 100–200 L of wastewater is produced from each 1 kg of textile product which involves various inorganic and organic elements and components (Akter and Islam, 2022a). Strong color, low metal, and suspended particle levels, high temperature, alkaline pH, low biodegradability in most circumstances, and high chemical oxygen demand (COD) are typical characteristics of the produced textile effluents (Tchamango et al., 2018; Ali and Mohammed, 2020).

The textile and printing industries employ a lot of synthetic dyes, which are frequently released into the environment without treatment. Azo dyes are the most commonly used synthetic dyes, making up around 70% of all dyes produced worldwide each year, which are very toxic dyes

and can cause cancer when being released into environment. This type of dyes have high resistance to microbial degradation because they have sulfonic (SO_3^-), hydroxyl (OH^-), and other electron-withdrawing functional groups in addition to at least one Azo group (-N=N-). Approximately, 50 k tons of textile dyes are being withdrawn into the environment every year due to the dyeing process (Sathishkumar et al., 2019; Irki et al., 2017). For this particular investigation, the dye selected in the present study was Methyl orange, a water-soluble Azo dye that possesses anionic properties and exhibits limited biodegradability (Hajiali et al., 2021; Maruthanayagam et al., 2020). Methyl orange (MO) is a common colorant used in the textile industry. It has been demonstrated that MO is extremely dangerous, can hurt the eyes, and may cause long-term ocular damage (Alardhi et al., 2023).

The contamination of natural water with aesthetically and toxically organic contaminants by the direct release of colored effluents which is a common occurrence in dyeing processes increase the need for treating these discharges before releasing into aquatic water. Biodegradation (Ye et al., 2023), adsorption (Purbasari et al., 2023; Fahad et al., 2017; Jawad and Naife, 2022), filtration (Liang et al., 2021), and coagulation-flocculation (El Mouhri et al., 2024; Gadekar and Ahammed, 2016) are some of the most conventional methods for treating textile wastewater. These methods have drawbacks, such as limited treatment efficiency, high operating costs, or secondary pollution from deposited sludge (Gökkuş et al., 2024).

Scientists have conducted extensive research and found that electrochemical methods are effective, cutting-edge technologies for eliminating certain pollutants from wastewater and mitigating environmental damage. Environmental compatibility, adaptability, energy efficiency, safety, selectivity, automation amenability, and cost-effectiveness are some of the advantages of employing electrochemical processes (Abbas and Abbas, 2022).

Numerous electrochemical methods are utilized to treat wastewater, including electroflotation (Da Mota et al., 2015), electro-Fenton (Mohammadi et al., 2024), electrodialysis (Scialdone, 2024), and electro-oxidation (Montañés et al., 2024) (Moreira et al., 2017).

The removal of contaminants from manufacturing and domestic wastewater has gained a lot of consideration in the field of electrocoagulation processes (EC) which is an environmentally friendly process that has been promoted as optimal due to its flexibility and compatibility (Salman et al., 2024). This low-cost method uses polyelectrolytes or salt polymers to interfere with the stability of suspended particles and emulsions in electrolytes (Issaka, 2024).

The utilization of EC process is based on using sacrificial anodes, usually composed of aluminum, iron, or nickel, these electrodes dissolve under controlled conditions, producing coagulant species in the water (Alardhi et al., 2023). Hydroxyl ions and hydrogen gas are produced at the cathode due to the reduction of water as shown in Equation 1, while the oxidation of water occurs on the anode as illustrated in Equation 2 (Tijana et al., 2021).

$$4H_2O + 4e^- \rightleftharpoons 2H_{2(g)} + 4HO^-_{(aq)} \quad (1)$$

$$H_2O \rightleftharpoons 4H^+_{(aq)} + O_{2(g)} + 4e^- \quad (2)$$

By utilizing Al as the sacrificial anode, Equation 3 illustrates its dissolution to produce Al ions (Jasim and Salman, 2024).

$$Al(s) \leftrightarrow Al^{+3}_{aq} + 3e^- \quad (3)$$

Complex precipitation kinetics takes place by reacting Al^{+3} with OH^- to form a variety of monomeric species, which ultimately change into $Al(OH)_3$ which is the basic coagulant as shown in Equation 4 (Bazrafshan et al., 2014; Liu et al., 2015).

$$Al^{+3}_{aq} + 3OH^-_{aq} \leftrightarrow Al(OH)_3 \quad (4)$$

Ni is utilized appropriately as a current collector and comes in a variety of forms, including mesh, wire, and foam. Ni foam is a lightweight material with a high porosity structure and an interwoven 3D scaffold of Ni metal. It is highly resistant to corrosion and has excellent electrical as well as thermal conductivity (Salleh et al., 2020). Nickel foam is an attractive material because of its high specific capacitance, well-defined electrochemical activity, and high stability. By using the metallic foam as a sacrificial anode in EC process have the advantages of adjusting catalytically the energy barrier to the electron transfer to produce metal hydroxides, and providing a continuous redox reaction due to its large surface area (Muthumanickam and Saravanathamizhan, 2021). The main reactions that occur at the electrodes involving Ni anode in the electrocoagulation process are illustrated in Equations 5 to 7 (Muthumanickam and Saravanathamizhan, 2021).

$$anode: Ni_{(s)} \rightarrow Ni^{2+}_{(aq)} + 2e^- \quad (5)$$

$$Ni^{2+}_{(aq)} + 2OH^-_{(aq)} \rightarrow Ni(OH)_{2(s)} \quad (6)$$

Overall reaction:

$$Ni_{(s)} + 2H_2O \rightarrow Ni(OH)_{2(s)} + H_{2(g)} \quad (7)$$

The overall reaction outlined in Equation 7 indicates a mechanism for the removal that involves the formation of $Ni(OH)_2$, which exhibits strong adsorption characteristics for dye attachment, leading to coagulation and precipitation. Various electrolytic forms, including NiOH, $Ni(OH)_2$, $Ni(OH)^{-3}$, $Ni(OH)^2{}_4$, and $Ni_4(OH)_4$ which may be produced depending on the pH levels of the aqueous medium, implying that the pH of the electrolyte governs the precipitation process. At elevated pH values, specific overpotentials can also lead to the formation of NiO, NiOOH, or $Ni(OH)_3$. The resulting $Ni(OH)_2$(s)/NiOOH manifests as sweep flocs with extensive surface areas, enhancing adsorption and facilitating the removal of pollutants. Nickel oxide was found to be a good adsorbent for treating various types of contaminants into wastewater (Muthumanickam and Saravanathamizhan, 2021).The main objective was to reduce the expense of treating wastewater with an EC process while utilizing the least amount of NaCl feasible. By using Ni foam electrode in the electrocoagulation (EC) technique to remove the MO dye from an aqueous solution, the authors hoped to further enhance the EC process advantages. Besides, examine the benefits of employing Al together with Ni foam as anodes in an EC system to overcome the leaching of Ni foam. The connecting method used was monopolar parallel which necessitates a smaller potential difference. Response surface methodology was used in the present study to optimize the controlled parameters.

MATERIALS AND METHODS

Chemicals

Distilled water was used to prepare all aqueous solutions, all chemicals used in experiments were of reagent grade, and there was no need for further purification. These chemicals were hydrochloric acid (HCl) (Thomas Baker Pvt. Ltd., India, with 37% purity), H_2SO_4 (central drug house (p) Ltd., new Delhi-110002 India, with purity of 98%), Methyl Orange (with a purity of 99.0 %), and NaCl (LOBA PVT Ltd., Mumbai India, with 99.5% purity).

Methyl orange properties and structure

Table 1 demonstrates the properties of Methyl Orange dye and Figure 1 displays its structure.

Table 1. Methyl orange properties

Molecular formula	$C_{14}H_{14}N_3NaO_3S$
Wavelength	464 nm
Solubility in water	5 g/L (at 20 °C)
Molar mass	327.33 g/mol

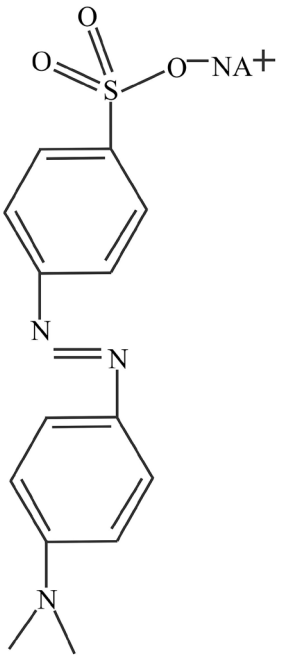

Figure 1. The molecular structure of methyl orange dye

Electrodes preparation

Prior activation of electrodes is an essential step before any EC process for eliminating any impurities or oxides layer on their surfaces. To achieve this, before each EC experiment, the NiF electrode was submerged in H_2SO_4 (1 M) for 10 min, and then rinsed with distilled water. Al and iron foam electrodes were rinsed with HCl solution (1 M) for at least 5 minutes and then washed with distilled water.

Dyes removal by EC system

The EC batch experiments were conducted in a cuboid-shaped glass reactor (17 cm in length, 17 cm in width, and 11 cm in height). The reactor was placed on a Heidolph hotplate stirrer (Germany), and the rotation speed was fixed at 200 rpm for continuous solution mixing. To detect the activity of Al and Ni foam in the EC system, primary experiments were accomplished by applying either two Al plates as anodes once or two Ni foam plates as anodes, or one plate of Al and

another one of Ni foam as anodes once. In all EC experiments, three electrodes of Fe foam were utilized as cathodes which are like Ni foam electrodes have a three dimensional structure which would enhance the solution mixing and enhance the production of H_2 gas resulting in increasing flotation. Therefore, the EC cells were composed of two anodes placed between three cathodes, and the distance between each two electrodes was set at 1.5 cm. The dimensions of the Al plate, Ni foam, or Fe foam were 6 cm in width and 14 cm in length, the thickness of the Al plate was 0.4 cm while the thickness each foam electrode was 1 cm. All electrodes were fitted vertically in the electrolytic cell with an active area of 156 cm^2 (based on four faces of Al and Ni foam anodes). The monopolar parallel electrodes were attached to a DC power supply (Yihua-305DI, China), and a digital multimeter (AS-MT890D, P.R.C) was used to measure the applied current to each anode (Al, and Ni foam). Then, 2 L of the aqueous solution was prepared by dissolving 100 mg/l of Methyl orange dye in deionized water (200 mg/l was added to 2 L to attain the required concentration of MO) with the required amount of NaCl (0.5, or 0.75 or 1 g/L, respectively). The selection of this range of NaCl was based on the analysis of different samples of wastewater which were taken from different textile effluents and the amount of NaCl was measured to perceive its concentration range and this range was approximately 1 g/L.

From previous studies, it can be concluded that one of the most controlling parameters in the efficiency of the EC process is the pH range which controls the rate of formation of different hydroxyl complexes of Al or Ni (Salman et al., 2024). Moreover, the ionic characteristic of dyes, the type of hydroxides produced, and consequently the mechanism of dye removal is governed by the pH range (Benaissa et al., 2016). In the present study, the experiments were accomplished at neutral pH (≈ 7) based on the outcomes of some previous studies which concluded that the highest removal efficiency of dyes was achieved at neutral pH (Liu et al., 2022; Salman et al., 2024; Jasim and Salman, 2024). Each experiment was conducted at room temperature (25 ± 2 °C), in duplicate, and the average value for the dye removal efficiency was determined. Each sample was analyzed with a UV–visible spectrophotometer (biotech Engineering Management CO. LTD, (UK) UV-9200). The calculation of Methyl orange concentration was based on the calibration curve at maximum wavelength (λ_{max}) of 464 nm. Figure 2 shows the experimental setup.

To measure the removal efficiency of Methyl Orange, Equation 8 was used as follows (Najim and Mohammed, 2018):

$$Methyl\ orange\ removal\ \% = \frac{(Mo-Mf)}{Mo} \times 100 \quad (8)$$

where: Mo is the initial MO dye concentration and M_f is its concentration after EC process in mg/L.

To detect the complete removal of dye not only its color, the COD must be measured also at the optimum conditions which was detected by using Lovibond® Water Testing reactor. Thus, 2

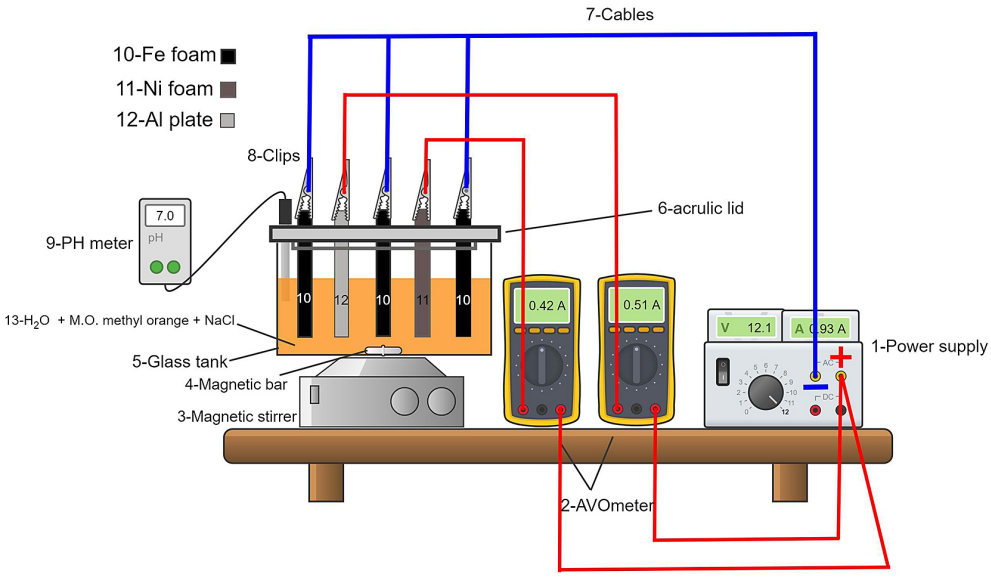

Figure 2. The schematic diagram of the EC system

ml of any treated sample was mixed with an oxidizing agent ($K_2Cr_2O_7$) and the testing would take place at 150 °C and continued 2 hours. The COD value was measured by a Photometer-System MD200.

To determine the consumed energy (SEC) in each experiment in (kWh/kg of MO dye), Equation 9 can be used (Hameed and Salman, 2024).

$$SEC = \frac{E.I.t}{(C_i - C_f)\,V} \times 1000 \qquad (9)$$

where: E is the voltage in (Volt), I is the current applied in (ampere), t is the time in (h), v indicates the volume of electrolytic solution in (L), and C_i, C_f indicate the initial and final concentration of MO dye, respectively in mg/L.

Primary experiment

As mentioned previously, primary experiments were conducted to show the advantages of applying two anodes of Al-NiF instead of Al-Al or NiF-NiF and how it affects the removal percentage of the MO Dye. This was accomplished at pH = 7, NaCl concentration of 1 g/L, and current density of 4 mA/cm^2.

Experimental design

Response surface methods (RSM) are multivariable procedures that can be applied theoretically to an experimental domain using a response function in a theoretical architecture and it is ideal in attaining optimum operating parameters (Theydan et al., 2024). In the present study, fifteen experiments were carried out based on the three-level Box-Behnken experimental design (BBD) for the EC system with adopting Al and NiF anodes. Table 2 displays the levels for each examined variable, and Table 3 illustrates the conditions of each experiment.

NiF electrode characterizations

Field emissive scanning electron microscopy (SEM, FEI-company) and energy dispersive X-ray (EDX, Bruker Company/Germany, with 100 A, 25 kV and XFlash-6110) would be used to

Table 2. EC process parameters and their levels for MO dye removal

Independent variable	Symbol	Unit	Low (-1)	Middle (0)	High (+1)
Current density	X1	mA/cm^2	4	6	8
NaCl concentration	X2	g/L	0.5	0.75	1
Time	X3	min	10	20	30

Table 3. Box-Behnken design for MO dye removal

Run	Coded value			Actual value		
	X1	X2	X3	Current density (mA/cm^2), X1	NaCl concentration (g/L), X2	Time (min), X3
1	0	0	0	6	20	0.75
2	-1	0	-1	4	20	0.50
3	1	-1	0	8	10	0.75
4	0	0	0	6	20	0.75
5	0	-1	1	6	10	1.00
6	-1	1	0	4	30	0.75
7	0	1	1	6	30	1.00
8	0	-1	-1	6	10	0.50
9	1	0	1	8	20	1.00
10	0	0	0	6	20	0.75
11	-1	-1	0	4	10	0.75
12	0	1	-1	6	30	0.50
13	1	1	0	8	30	0.75
14	-1	0	1	4	20	1.00
15	1	0	-1	8	20	0.50

detect the surface morphology and elements composition of NiF electrode before and after its utilization as anode in the EC process.

RESULTS AND DISCUSSION

Effect of electrode type on EC process

Working on three different sets of anodes electrodes under the same conditions and examining the MO removal percentage results was necessary to indicate the efficiency of each type of anodes. Therefore, primary experiments were conducted at 4 mA/cm^2, 1 g/L of NaCl, pH =7 within 30 min of electrolysis by using two Al anodes, or two NiF anodes, or Al-NiF anodes. The cathode electrodes were three iron foam, and Table 4 illustrates the results of these experiments.

Using Al-Al anodes in the EC system showed the lower MO dye removal percentages and the higher removal percentages was reached at approximately 40 min where pitting corrosion was appeared on the Al electrodes after this time of electrolysis. However, The EC experiment with two Ni foam electrodes showed higher MO dye removal percentages which demonstrated that Ni foam anodes were very effective, but also a green color in the electrolytic solution appeared after 30 min due to the leaching of Ni foam electrodes, which is a major drawback. Finally, combining one Al anode with another anode of Ni foam was examined to attain the advantages of both electrodes without their drawbacks. As stated in Table 4, a high MO dye removal percentage was obtained with these two anodes without any green color in the solution or pitting corrosion on the surface of Al plate, which indicated the advantages of combining these anodes. Therefore, in the following experiments to detect the effect of different parameters on EC system, the anodes utilized were Al and Ni foam, besides three Fe foam electrodes as cathodes.

BBD statistical analysis results

Development of regression model

The regression model equations produced by MINITAB-19 software are displayed in Equation 10 as follows, and Table 5 presents the

Table 4. Results of MO dye removal % at different anodes setups

Time, min	MO dye removal % at 4 mA/cm^2, pH= 7, and NaCl Conc.= 1 g/L		
	Al- Al anodes	NiF- NiF anodes	Al- NiF anodes
10	23.63%	73.00%	75.34%
20	30.49%	83.30%	86.09%
30	48.88%	86.45%	88.46%

Table 5. Actual and predicted values for MO dye removal% and energy consumption (SEC)

Exp. No.	C.D., mA/cm^2	Time, min	NaCl Conc., g/L	Actual MO dye Re %	Predicted MO dye Re %	E, volt	SEC (kWh/kg MO dye)
1	6	20	0.75	85.97	85.31	10.1	26.28
2	4	20	0.5	75.345	75.98	9.9	17.12
3	8	10	0.75	88.78	89.88	10.3	17.00
4	6	20	0.75	84.52	85.31	10.1	28.42
5	6	10	1	92.05	91.59	8	10.09
6	4	30	0.75	86.11	85.04	7.3	17.41
7	6	30	1	93.12	93.27	7.1	26.44
8	6	10	0.5	78.32	78.20	7.4	9.22
9	8	20	1	96.497	95.89	8.6	23.92
10	6	20	0.75	85.387	85.31	7.4	23.40
11	4	10	0.75	78.32	77.84	8.7	6.07
12	6	30	0.5	87.18	87.67	4.3	16.28
13	8	30	0.75	93.327	93.83	8.7	36.86
14	4	20	1	88.07	89.03	5.9	8.34
15	8	20	0.5	90.9	89.96	17.5	61.94

experimental results of MO dye removal percentages, and the predicted MO dye removal % and SEC which were estimated based on Equation 10 and Equation 9, respectively.

MO dye Rem % = 41.6 + 4.02 C.D. + + 0.845 time + 14.6 NaCl Conc.+0.172 C.D. × × C.D.+ 0.00653 time × time+ 27.55 NaCl Conc. × × NaCl Conc. - 0.0405 C.D. × time-3.56 C.D. × NaCl Conc.- 0.779 time × NaCl Conc. (10)

Analysis of variance (ANOVA)

ANOVA is a useful technique for process improvement and comprehension, since it can predict the impact of factors and their interactions on the result (Jasim and Salman, 2024). The ANOVA findings are displayed in Table 6; where P-value is a statistical measure of probability and F-value is Fisher value. A high F-value (more than 4) indicates that the regression equation can explain the variation in the solution. When a model's p-value is less than 0.05, it is deemed statistically significant (Ozyurt et al., 2017). Table 6 demonstrates that the model can effectively characterize the elimination process and that it was highly significant for MO degradation with F and P values of 39.99 and 0.000, respectively. High correlation coefficient R^2 value of 98.63% was acquired, and the contribution percentages showed that the sequence of parameters due to their high effect on MO dye removal % were current density, NaCl concentration, and time.

Effect of studied parameters on EC process

To emphasize the effect of the studied parameter on the removal efficiency of MO dye, a 3D surface plot based on RSM analysis and histogram plot were considered. Figure 3 displays the effect of current density and electrolysis time onto EC process efficiency. First of all, it must be declared that the applied current was divided equally between Al and NiF electrodes. Not surprisingly, it is clear that increasing current density resulted in increasing MO dye removal. For an example, based on the results of Table 5, by comparing the results of experiments 2 and 15, it can be noted that at NaCl conc. = 0.5 g/L and within 20 minutes of electrolysis, the increase in current density from 4 to 8 mA/cm^2 resulted in increasing MO dye removal % from 75.345 to 90.9%. Additionally, it can be noticed that when increasing current density from 4 to 6 mA/cm^2 at pH = 7 and 0.75 g/L of NaCl within 30 min of electrolysis, MO dye removal percentage increased from 85.04 to 93.83%. According to Faradays' law $m = [ItM/zF]$), the increase of current density would enhance the generation of more electrode ionic species (Al^{3+} and

Table 6. ANOVA results for MO dye removal

Source	DF	Seq SS	Contribution	Adj SS	Adj MS	F-Value	P-Value
Model	9	502.799	98.63%	502.799	55.867	39.99	0.000
Linear	3	459.335	90.10%	459.335	153.112	109.60	0.000
C.D.	1	216.934	42.55%	216.934	216.934	155.28	0.000
Time	1	61.977	12.16%	61.977	61.977	44.36	0.001
NaCl conc.	1	180.424	35.39%	180.424	180.424	129.15	0.000
Square	3	12.961	2.54%	12.961	4.320	3.09	0.128
C.D.*C.D.	1	1.006	0.20%	1.751	1.751	1.25	0.314
Time*time	1	1.007	0.20%	1.575	1.575	1.13	0.337
NaCl conc.*NaCl conc.	1	10.948	2.15%	10.948	10.948	7.84	0.038
2-Way Interaction	3	30.502	5.98%	30.502	10.167	7.28	0.028
C.D.*time	1	2.629	0.52%	2.629	2.629	1.88	0.228
C.D.*NaCl conc.	1	12.702	2.49%	12.702	12.702	9.09	0.030
time*NaCl conc.	1	15.171	2.98%	15.171	15.171	10.86	0.022
Error	5	6.985	1.37%	6.985	1.397		
Lack-of-Fit	3	5.920	1.16%	5.920	1.973	3.71	0.220
Pure Error	2	1.065	0.21%	1.065	0.532		
Total	14	509.784	100.00%				
Model summary	S	R-sq	R-sq(adj)	PRESS	R-sq(pred)	AICc	BIC
	1.18196	98.63%	96.16%	97.1231	80.95%	141.10	60.89

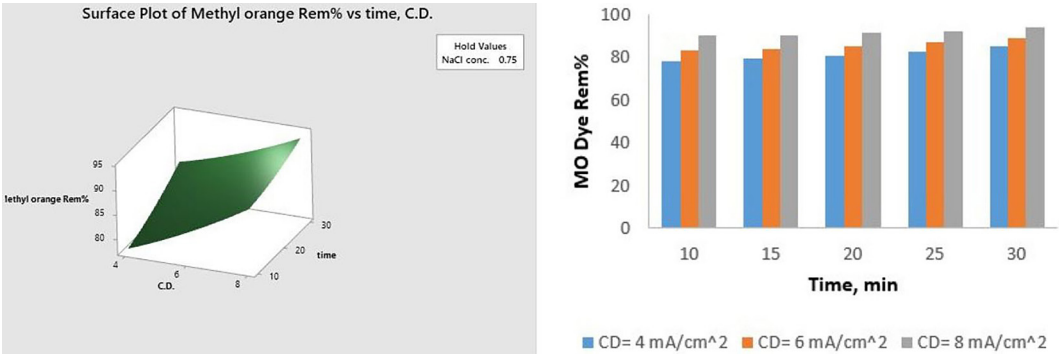

Figure 3. Effect of current density with time at NaCl conc. = 0.75 g/L on MO dye removal, (a) 3D surface plot, (b) Histogram plot

Ni^{+2}) onto the anodes which would increase the production of more $Al(OH)_3$ and $Ni(OH)_2$ flocs in the solution and consequently an enhancement in the MO dye removal (Jasim and Salman, 2024; Abbas et al., 2022).

Furthermore, increasing current density would increase the rate of H_2 and O_2 bubble generation which intensely impacts the rate of flotation, solution mixing, and mass transfer at the electrodes. In fact, current density is one of the vital operational parameters which must be taken into consideration for the design of any EC setup; hence, it not only influences the system response time but also strongly affects the governing contaminant separation method. However, this key parameter must be controlled to avoid the decrease in current efficiency and the waste in electrical energy (Irki et al., 2017; Kul et al., 2020).

Another vital parameter must be controlled in EC process is electrolysis time, hence it is essential to remember that operational costs are governed by reaction time. Thus, for effective treatment at the lowest feasible cost, a reaction time value needs to be selected. As it was stated in Table 5, increasing electrolysis time from 10 to 30 min resulted in increasing the MO dye removal percentages from 88.78 to 93.327% at 8 mA/cm^2 and 0.75 g/L of NaCl. On the basis of Faradays' law, higher electrolysis time means higher number of produced metal ions in the electrolyte and consequently a higher number of metal hydroxides.

The addition of different electrolytes like NaCl, Na_2SO_4, and KCl can directly impact the efficiency of the EC process. In the present study, NaCl was chosen as the main electrolyte due to its natural presence in wastewater of different industries and especially in textile industries due to its utilization as an absorbent of dye molecules in the cloth fibers besides its high efficiency in increasing the conductivity of electrolytic solution (Salman et al., 2024). Furthermore, the presence of Cl ions prevents the negative of Ca ions that naturally exist in all the types of wastewater (Mohammed et al., 2021).Therefore, it is commonly to consider the addition of NaCl as one of the main parameters that govern the efficiency of EC process. Figure 4 shows the effect of NaCl addition and it can be predicted from Table 5 by comparing the results of runs 2 and 14 that at 4 mA/cm^2 and within 20 min of electrolysis, increasing the NaCl concentration from 0.5 to 1 g/L, the MO dye removal efficiency was increased from 75.345 to 88.07%. This also can be explained by the fact that the addition of NaCl to the bulk solution can anodically produce chlorine species like hypochlorous acid (HOCl) and hypochlorite ions (-OCl) which enhance the indirect electrolysis and converts organic contaminants into H_2O and CO_2 (Muthumanickam and Saravanathamizhan, 2021; Titchou et al., 2020). Equations 11–14 explain the main reactions by adding NaCl to the bulk solution (Jasim and Salman, 2024; Titchou et al., 2020). However, in neutral bulk solution, HOCl is the main chlorine species which would be produced and is more active in eliminating pollutants than hypochlorite ions (Jasim and Salman, 2024).

$$2Cl^- \rightarrow Cl_2 + +2e^- \quad (11)$$

$$Cl_2 + H_2O \rightarrow HOCl + H^+ + Cl^- \quad (12)$$

$$HOCl \rightarrow H^+ + OCl^- \quad (13)$$

$$Dye + OCl^- \rightarrow \text{Intermediates} \rightarrow \rightarrow CO_{2(g)} + H_2O + Cl^- \quad (14)$$

The results of present work in agreement with many previous studies (Titchou et al., 2020; Muthumanickam and Saravanathamizhan, 2021b; Irki et al., 2018; Irki et al., 2017), but it succeeded

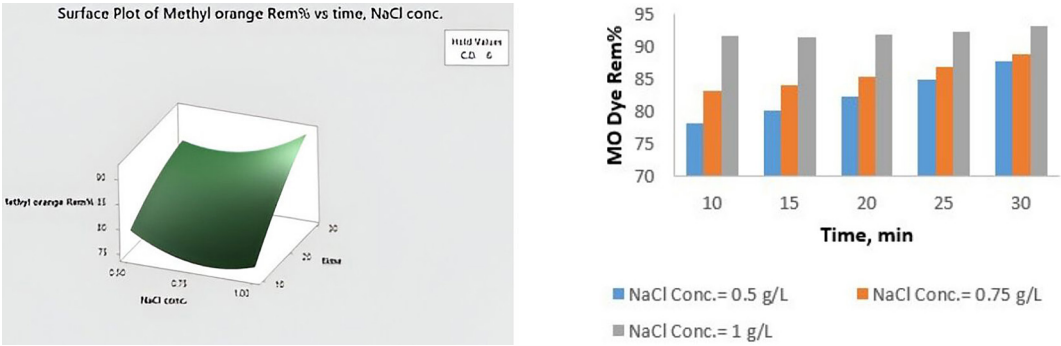

Figure 4. Effect of NaCl with time on MO dye removal at 6 mA/cm^2, (a) 3D surface plot, (b) histogram plot

in removing MO dye with low amounts of NaCl in comparison with many previous studies.

As anticipated, the results of consumed energy (SEC) in Table 5 confirmed that it increased along with current density. It can be emphasized that the consumed energy increased from 17.12 to 61.94 kWh/kg of MO dye as the current density increased from 4 to 8 mA/cm^2 at NaCl concentration of 0.5 g/L and 20 min of electrolysis. Nevertheless, SEC increase decreased with NaCl increase, as illustrated in Table 5, which can be observed in runs 9 and 15, where it decreased from 61.94 to 23.92 kWh/kg of MO dye at 8 mA/cm^2, time = 20 min as an increase in NaCl concentration was observed from 0.5 to 1 g/L, respectively.

This decrease in consumed energy by increasing NaCl concentration can be explained by the fact that higher NaCl concentration would decrease the insulating layer on the anodes, enhance the electrolyte conductivity, reduce the voltage, and decrease the energy consumption as a result (Irki et al., 2018).

Optimization and confirmation experiments

As the main goal of this study is to acquire the maximum MO dye removal %, the maximum target was adopted in the present study. In Table 7, optimum conditions from the desirable function were 8 mA/cm^2, 1 g/L of NaCl, and time of 30 min. Two experiments were accomplished by adopting these optimum conditions, and the results are illustrated in Table 7. The MO dye removal efficiency was 97.74 % after 30 min and COD measuring was achieved for initial and final samples of these two experiments at these optimum conditions and it was found that the initial and final COD values were around 51 mg/L which considered acceptable values. To emphasize the efficiency of current study with previous studies investigated the removal of MO dye; Table 8 illustrates the results of some previous studies besides those obtained in the present study. It can be concluded that the present EC system can be considered as a promising system for efficient removal of MO dye with moderate conditions.

Characterization of the NiF electrode

Figure 5 displays the morphological structure of the NiF electrode before utilizing it as anode in the EC system and after 15 experiments of electrocoagulation of MO dye. As depicted in Figure 5A1 and 5A2, the Ni foam before experiments had a smooth surface, cross-linked, 3D porous structure and has a tiny diameter (hole and strand). Because of its porous structure, Ni foam has a huge surface area. Greater charge transfer, stronger pseudo capacitance characteristics, and fewer blockages between the active material and electrolyte can result from the larger surface area (Salleh et al., 2020). As a result of this 3D, porous structure of the NiF electrode, it was very effective as an anode in the EC system. Figures 5B1 and 5B2 shows its surface after 15 experiments of an EC process and it is easy to predict the change in its structure due to the Ni ions dissolution and leaching during the EC experiments.

Table 7. Results of MO dye removal efficiency and SEC at optimum conditions

Run No.	C.D. (mA/cm^2)	NaCl conc. (g/L)	Time (min)	MO Removal %	E (Volt)	Average removal%	SEC (kWh/kg of MO)
1	8	1	30	97.85	8.7	97.74	36.30
2	8	1	30	97.62	8.6		35.88

Table 8. Results of the present study with some previous studies for MO dye removal

Electrodes	pH	Time, min	Electrolyte type	Current density and Voltage	MO dye Rem%	Reference
Al-Fe	5–7	50	NaCl, 1 g/L	20 volt	97%	(Ren et al., 2018)
Al-Fe	3–5	20	Na_2SO_4	10 mA/cm^2, 6–30 volt	92%	(Karagözoğlu and Malkoç, 2023)
SS sieve box - Fe	7	60	NaCl, 1 g/L	40 volt	93.10%	(Sorayyaei et al., 2021)
Fe-Fe	7.25	12	NaCl, 1.6 g/L	6.4 mA/cm^2	95%	(Irki et al., 2017)
4 Fe	4–5	32	Fe^{2+}, 0.2 mM	0.4 mA/cm^2	82.4%	(Akter and Islam, 2022b)
Al-Fe	7.4	20	NaCl	150 mA/cm^2, 4.4 volt	94%	(Pi et al., 2014)
Fe-Fe	8	40	-	3 mA/cm^2, 0–30 volt	97%	(Abbas et al., 2022b)
Al-NiF	7	30	NaCl, 1 g/L	8 mA/cm^2	97.74%	Present study

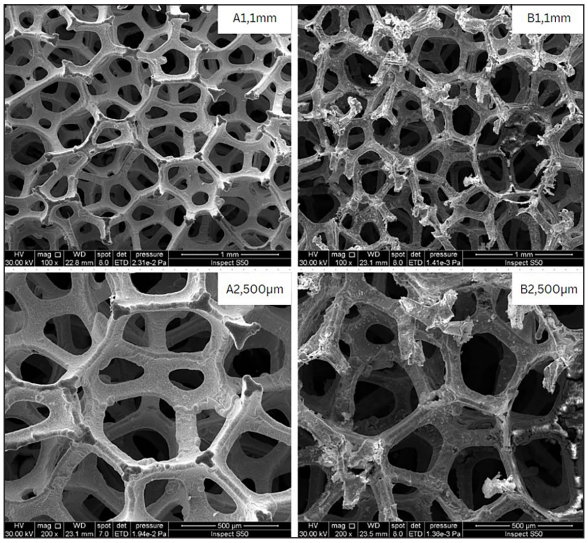

Figure 5. FESEM image of the NiF electrode at different magnifications (1 refers to 100×, and 2 refers to 200×); A: before EC process, and B: after EC process

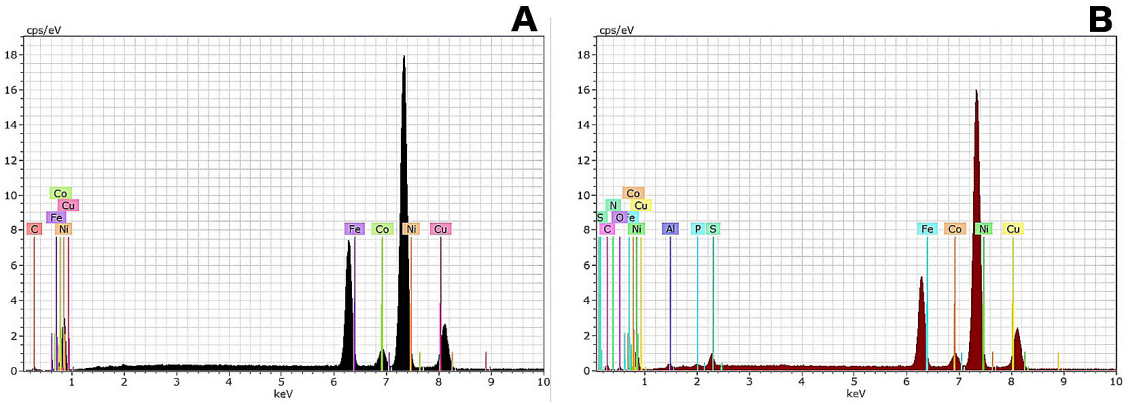

Figure 6. EDX images of the NiF electrode; A: before EC process, and B: after EC process

The EDX results of the NiF anodes before and after the EC process are depicted in Figure 6. It can be predicted that Ni has the higher percentage of the total composition in addition to minor elements like Fe, Co, Cu, and C, as shown in Figure 6A, while Figure 6B shows the EDX results of NiF after EC experiments and also it can be noted that Ni had the higher percentage of the total compositions besides small percentages of Fe, Co, Cu, C, Al, and S.

CONCLUSIONS

In this work, the main goal was to detect the efficiency of an EC system in eliminating MO dye in the presence of Ni foam and aluminum anodes besides Fe foam as cathodes. The results indicated that an EC system with Al-NiF electrodes was more efficient than one of Al-Al or NiF-NiF which reduced the required time of removal in the case of using the Al-Al anodes and eliminate the leaching of Ni in the case of utilizing the NiF-NiF anodes. The impact of current density, NaCl concentration, and time on the efficiency of the EC system was optimized with response surface methodology. It was concluded that current density had the highest impact on the EC process followed by NaCl concentration, and the electrolysis time has the lower impact. The higher MO dye removal percentage was 97.74% at 8 mA/cm^2, 1 g/L of NaCl within 30 min of electrolysis with a consumed energy of 36.09 kWh/kg of MO dye. The present EC system succeeded effectively in removing the MO dye with lower values of time and the NaCl concentration in comparison with many previous studies. The 3D and porous structure of the NiF and Fe foam electrodes enhanced dramatically the EC process due to the high surface area of these electrodes which enhanced the production of H_2 and O_2 gases and consequently enhanced the mass transfer, mixing of solution, and flotation rate.

REFERENCES

1. Abbas, R.N., Abbas, A.S. 2022a. Kinetics and energetic parameters study of phenol removal from aqueous solution by electro-Fenton advanced oxidation using modified electrodes with PbO2 and graphene. Iraqi Journal of Chemical and Petroleum Engineering, 23(2), 1–8. https://doi.org/10.31699/ijcpe.2022.2.1
2. Abbas, S.H., Younis, Y.M., Rashid, K.H., Khadom, A.A. 2022b. Removal of methyl orange dye from simulated wastewater by electrocoagulation technique using Taguchi method: kinetics and optimization approaches. Reaction Kinetics, Mechanisms and Catalysis, 135, 2663–2679. https://doi.org/10.1007/s11144-022-02269-9
3. Akter, S., Islam, M.S. 2022. Effect of additional Fe2+ salt on electrocoagulation process for the degradation of methyl orange dye: An optimization and kinetic study. Heliyon, 8(8), e10176. https://doi.org/10.1016/j.heliyon.2022.e10176
4. Alardhi, S.M., Fiyadh, S.S., Salman, A.D., Adelikhah, M. 2023. Prediction of methyl orange dye (MO) adsorption using activated carbon with an artificial neural network optimization modeling. Heliyon, 9(1), e12888. https://doi.org/10.1016/j.heliyon.2023.e12888
5. Ali, H.Q., Mohammed, A.A. 2020. Elimination of congo red dyes from aqueous solution using *Eichhornia crassipes*. Iraqi Journal of Chemical and Petroleum Engineering, 21(4), 21–32. https://doi.org/10.31699/ijcpe.2020.4.3
6. Bassyouni, D., Ali, S., Abdel-Aziz, M.H., Elashtoukhy, E. 2023. Electrocoagulation technique and statistical analysis for treatment of real effluent from the pulp and paper industry. International Journal of Electrochemical Science, 18(12), 100389. https://doi.org/10.1016/J.IJOES.2023.100389
7. Bazrafshan, E., Mahvi, A.H., Zazouli, M.A. 2014. Textile wastewater treatment by electrocoagulation process using aluminum electrodes. Iranian journal of health sciences, 2(1), 16–29. https://doi.org/10.18869/acadpub.jhs.2.1.16
8. Benaissa, F., Kermet-Said, H., Moulai-Mostefa, N. 2016. Optimization and kinetic modeling of electrocoagulation treatment of dairy wastewater. Desalination and Water Treatment, 57(13), 5988–5994. https://doi.org/10.1080/19443994.2014.985722
9. De Oliveira Da Mota, I., De Castro, J.A., De Góes Casqueira, R., De Oliveira Junior, A.G. 2015. Study of electroflotation method for treatment of wastewater from washing soil contaminated by heavy metals. Journal of Materials Research and Technology, 4(2), 109–113. https://doi.org/10.1016/j.jmrt.2014.11.004
10. El Mouhri, G., Elmansouri, I., Amakdouf, H., Belhassan, H., Kachkoul, R., El oumari, F.E., Merzouki, M., Lahrichi, A. 2024. Evaluating the effectiveness of coagulation–flocculation treatment on a wastewater from the Moroccan leather tanning industry : An ecological approach. Heliyon, 10(5), e27056. https://doi.org/10.1016/j.heliyon.2024.e27056
11. Fahad, B.M., Ali, N.S., Hameed, T.T. 2017. the influence of eggshell particle sizes on the adsorption of organic dye. Iraqi Journal of Chemical and Petroleum Engineering 18(1), 111–120. https://doi.org/10.31699/IJCPE.2017.1.9
12. Gadekar, M.R., Ahammed, M.M. 2016. Coagulation/flocculation process for dye removal using water treatment residuals: modelling through artificial neural networks. Desalination and Water Treatment, 57(55), 26392–26400. https://doi.org/10.1080/19443994.2016.1165150
13. Gökkuş, Ö., Brillas, E., Sirés, I. 2024. Sequential use of a continuous-flow electrocoagulation reactor and a (photo)electro-Fenton recirculation system for the treatment of Acid Brown 14 diazo dye. Science of the Total Environment, 912(20 February), 169143.

https://doi.org/10.1016/j.scitotenv.2023.169143

14. Hajiali, M., Farhadian, M., Aaki, S., Davari, N. 2021. Application of $TiO_2/ZnFe_2O_4$/glycine nanocatalyst to the treatment of methyl orange dye from aqueous solution: Impacts of dissolved mineral salts on dye removal efficiency. Scientia Iranica, 28(3), 1464–1477. https://doi.org/10.24200/sci.2021.56415.4715
15. Hameed, Z.M., Salman, R.H. 2024. Elimination of methyl orange dye with three dimensional electro-Fenton and sono-electro-Fenton systems utilizing copper foam and activated carbon. Ecological Engineering & Environmental Technology, 25(10), 44–59. https://doi.org/10.12912/27197050/191199
16. Irki, S., Ghernaout, D., Naceur, M.W. 2017. Decolourization of methyl orange (MO) by electrocoagulation (EC) using iron electrodes under a magnetic field (MF). Desalination and Water Treatment, 79(June), 368–377. https://doi.org/10.5004/dwt.2017.20797
17. Irki, S., Ghernaout, D., Naceur, M.W., Alghamdi, A., Aichouni, M. 2018. Decolorizing methyl orange by fe-electrocoagulation process – A mechanistic insight. International Journal of Environmental Chemistry, 2(1), 18-28. https://doi.org/10.11648/j.ijec.20180201.14
18. Issaka, E. 2024. From complex molecules to harmless byproducts: Electrocoagulation process for water contaminants degradation. Desalination and Water Treatment, 319(July), 100532. https://doi.org/10.1016/j.dwt.2024.100532
19. Jasim, R.A., Salman, R.H. 2024. Use of nano Co-Ni-Mn composite and aluminum for removal of artificial anionic dye congo red by combined system. Ecological Engineering and Environmental Technology, 25(7), 133–149. https://doi.org/10.12912/27197050/188266
20. Jawad, N., Naife, T.M. 2022. Mathematical modeling and kinetics of removing metal ions from industrial wastewater. Iraqi Journal of Chemical and Petroleum Engineering, 23(4), 59–69. https://doi.org/10.31699/ijcpe.2022.4.8
21. Karagözoğlu, M.B., Malkoç, R. 2023. Optimization of operating parameters in the removal of synthetic textile dyestuff with the electrocoagulation process. Iranian Journal of Chemistry and Chemical Engineering, 42(5), 1553–1573. https://doi.org/10.30492/IJCCE.2022.555487.5381
22. Kul, M., Oskay, K.O., Erden, F., Akça, E., Katirci, R., Köksal, E., Akinci, E. 2020. Effect of process parameters on the electrodeposition of zinc on 1010 Steel: Central composite design optimization. International Journal of Electrochemical Science, 15(10), 9779–9795. https://doi.org/10.20964/2020.10.19
23. Liang, C., Wei, D., Zhang, S., Ren, Q., Shi, J., Liu, L. 2021. Removal of antibiotic resistance genes from swine wastewater by membrane filtration treatment. Ecotoxicology and Environmental Safety, 210(March), 111885. https://doi.org/10.1016/j.ecoenv.2020.111885
24. Liu, Y., Li, C., Bao, J., Wang, X., Yu, W., Shao, L. 2022. Degradation of azo dyes with different functional groups in simulated wastewater by electrocoagulation. Water, 14(1), 123. https://doi.org/10.3390/w14010123
25. Liu, Y.J., Lo, S.L., Liou, Y.H., Hu, C.Y. 2015. Removal of nonsteroidal anti-inflammatory drugs (NSAIDs) by electrocoagulation-flotation with a cationic surfactant. Separation and Purification Technology, 152(25 September), 148–154. https://doi.org/10.1016/j.seppur.2015.08.015
26. Maruthanayagam, A., Mani, P., Kaliappan, K., Chinnappan, S. 2020. In vitro and in silico studies on the removal of methyl orange from aqueous solution using *Oedogonium* subplagiostomum AP1. Water, Air, & Soil Pollution, 231. https://doi.org/10.1007/s11270-020-04585-z
27. Mohammadi, F., Rahimi, S., Amin, M.M., Dehdashti, B., Janati, M. 2024. Hybrid ANFIS-ant colony optimization model for prediction of carbamazepine degradation using electro-Fenton process catalyzed by $Fe@Fe_2O_3$ nanowire from aqueous solution. Results in Engineering, 23(September), 102447. https://doi.org/10.1016/j.rineng.2024.102447
28. Mohammed, S.J., M-Ridha, M.J., Abed, K.M., Elgharbawy, A.A.M. 2021. Removal of levofloxacin and ciprofloxacin from aqueous solutions and an economic evaluation using the electrocoagulation process. International Journal of Environmental Analytical Chemistry, 103(16), 3801–3819. https://doi.org/10.1080/03067319.2021.1913733
29. Montañés, M.T., García-Gabaldón, M., Giner-Sanz, J.J., Mora-Gómez, J., Pérez-Herranz, V. 2024. Effect of the anode material, applied current and reactor configuration on the atenolol toxicity during an electro-oxidation process. Heliyon, 10(5), e27266. https://doi.org/10.1016/j.heliyon.2024.e27266
30. Moreira, F.C., Boaventura, R.A.R., Brillas, E., Vilar, V.J.P. 2017. Electrochemical advanced oxidation processes: A review on their application to synthetic and real wastewaters. Applied Catalysis B: Environmental, 202(March), 217-261. https://doi.org/10.1016/j.apcatb.2016.08.037
31. Muthumanickam, K., Saravanathamizhan, R. 2021. Electrochemical treatment of dye wastewater using nickel foam electrode. Journal of Electrochemical Science and Engineering 11, 209–215. https://doi.org/10.5599/jese.1011
32. Najim, A.A., Mohammed, A.A. 2018. Biosorption of Methylene Blue from Aqueous Solution Using Mixed Algae. Iraqi Journal of Chemical and Petroleum Engineering, 19(4), 1–11. https://doi.

org/10.31699/ijcpe.2018.4.1

33. Ozyurt, B., Camcıoğlu, Ş., Hapoglu, H. 2017. A consecutive electrocoagulation and electro-oxidation treatment for pulp and paper mill wastewater. Desalination and Water Treatment, 93, 214–228. https://doi.org/10.5004/dwt.2017.21257
34. Pi, K.W., Xiao, Q., Zhang, H.Q., Xia, M., Gerson, A.R. 2014. Decolorization of synthetic Methyl Orange wastewater by electrocoagulation with periodic reversal of electrodes and optimization by RSM. Process Safety and Environmental Protection, 92, 796–806. https://doi.org/10.1016/j.psep.2014.02.008
35. Purbasari, A., Ariyanti, D., Fitriani, E. 2023. Adsorption of Methyl Orange Dye by Modified Fly Ash-Based Geopolymer–Characterization, Performance, Kinetics and Isotherm Studies. Journal of Ecological Engineering, 24(3), 90–98. https://doi.org/10.12911/22998993/157541
36. Ren, L.M., Li, H.Q., Wang, Y. 2018. Treatment of high strength methyl orange wastewater by electrocoagulation with periodic reversal of electrodes: Effect of voltage variation. Desalination Water Treat 135, 258–267. https://doi.org/10.5004/dwt.2018.23261
37. Salleh, N.A., Kheawhom, S., Mohamad, A.A. 2020. Characterizations of nickel mesh and nickel foam current collectors for supercapacitor application. Arabian Journal of Chemistry 13, 6838–6846. https://doi.org/10.1016/j.arabjc.2020.06.036
38. Salman, R.H., Khudhair, E.M., Abed, K.M., Abbas, A.S. 2024. Removal of E133 brilliant blue dye from artificial wastewater by electrocoagulation using cans waste as electrodes. Environmental Progress and Sustainable Energy, 43(2), e14292. https://doi.org/10.1002/ep.14292
39. Sathishkumar, K., AlSalhi, M.S., Sanganyado, E., Devanesan, S., Arulprakash, A., Rajasekar, A. 2019. Sequential electrochemical oxidation and bio-treatment of the azo dye congo red and textile effluent. Journal of Photochemistry and Photobiology B: Biology, 200, 111655. https://doi.org/10.1016/j.jphotobiol.2019.111655
40. Scialdone, O. 2024. Electrochemical synthesis of chemicals and treatment of wastewater promoted by salinity gradients using reverse electrodialysis and assisted reverse electrodialysis. Current Opinion in Electrochemistry, 43, 101421. https://doi.org/10.1016/j.coelec.2023.101421
41. Sorayyaei, S., Raji, F., Rahbar-Kelishami, A., Ashrafizadeh, S.N. 2021. Combination of electrocoagulation and adsorption processes to remove methyl orange from aqueous solution. Environmental Technology & Innovation, 24, 102018. https://doi.org/10.1016/j.eti.2021.102018
42. Tchamango, S.R., Kamdoum, O., Donfack, D., Babale, D. 2018. Comparison of electrocoagulation and chemical coagulation processes in the treatment of an effluent of a textile factory. Journal of Applied Sciences and Environmental Management, 21, 1317. https://doi.org/10.4314/jasem.v21i7.17
43. Theydan, S.K., Mohammed, W.T., Haque, S.M. 2024. Three-dimensional electrocoagulation process optimization employing response surface methodology that operated at batch recirculation mode for treatment refinery wastewaters. Iraqi Journal of Chemical and Petroleum Engineering, 25(1), 59–74. https://doi.org/10.31699/ijcpe.2024.1.6
44. Tijana, J., NeNa, V., Milica, P., Slobodan, N., Danijelać, B., Miljana, R., Aleksandar, B. 2021. Mechanism of the electrocoagulation process and its application for treatment of wastewater: A review. Advanced Technologies, 10(1), 63–72. https://doi.org/10.5937/savteh2101063J
45. Titchou, F.E., Afanga, H., Zazou, H., Ait Akbour, R., Hamdani, M. 2020. Batch elimination of cationic dye from aqueous solution by electrocoagulation process. Mediterranean Journal of Chemistry, 10, 1–12. https://doi.org/10.13171/mjc10102001201163mh
46. Ye, Q., Wu, H., Li, J., Huang, Y., Zhang, M., Yi, Q., Yan, B. 2023. Preparation of 1,8-dichloroanthraquinone/graphene oxide/poly (vinylidene fluoride) (1,8-AQ/GO/PVDF) mediator membrane and its application to catalyzing biodegradation of azo dyes. Ecotoxicology and Environmental Safety, 268, 115681. https://doi.org/10.1016/j.ecoenv.2023.115681